

Fig. 2. Pore size distribution of the bamboo-derived GAC prepared at different KOH/C mass ratios (a) and activation temperatures (b).

(Fig. 1a) were attributed to the enlarged pores obtained. However, the activated carbons prepared under the severe activation condition would break easily in the adsorption process. Fig. 2b presents the pore size distribution of activated carbons prepared at the activation temperature from 700 °C to 900 °C. Their overall pore size distribution of activated carbons did not change obviously. However, it still can be seen that the pore volume in the size range of 1–2 nm decreased, while the pore volume in the range of 2–4 nm increased with increasing activation temperatures, indicating that the pores were enlarged at high temperatures. The enlarged pores should be responsible for the enhanced adsorption of PFOS on the activated carbons (Fig. 1b). Their macropore size distributions were also measured (Fig. S1), and the pore volume increased with increasing KOH/C ratio and activation temperature. Although the macropores had high volume, they had low contribution to the adsorption of PFOS due to the low surface area. The specific surface areas of the activated carbons prepared at different KOH/C ratios and activation temperatures are shown in Fig. 3. The surface area increased with increasing KOH/C ratios, but it first increased and then decreased with increasing activation temperature, implying that the adsorbed amounts of PFOS on the activated carbons were not completely consistent with their surface areas, and the available pores in the activated carbon were more important for PFOS adsorption. Although some pores were enlarged with increasing KOH/C ratio and activation temperature, the SSA still increased in most cases since some new pores were also produced.

3.3. SEM observation

Fig. 4 shows the SEM images of the carbonized bamboo and bamboo-derived activated carbon. Some pores less than 10 μm can be observed in the cross section of the carbonized bamboo (Fig. 4a). After the activation at the KOH/C ratio of 4 at 900 °C, most of the pores were enlarged to the range of 10–20 μm (Fig. 4c). These big pores were parallel to the cellulose fibers (Fig. 4b), favorable for the diffusion of PFOS/PFOA into the granular adsorbent. Some

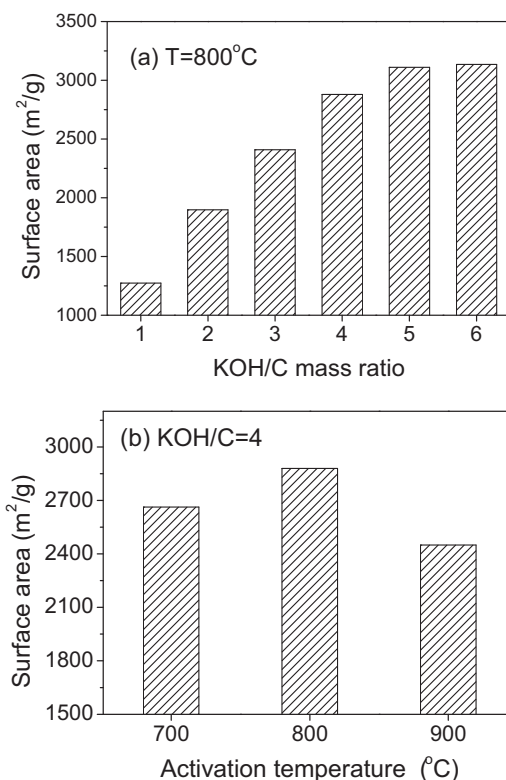


Fig. 3. Effects of KOH/C mass ratio and activation temperature on the specific surface area of the bamboo-derived GAC.

nano-sized pores were found on the walls of micron-sized pores (Fig. 4d), but many pores of less than 100 nm invisible on this SEM image should exist due to the large surface area (2450 m²/g) of this activated carbon, which may be mainly responsible for PFOS adsorption.

3.4. Adsorption kinetics

The adsorption equilibrium of PFOS and PFOA on the bamboo-derived GAC was almost obtained within 24 h (Fig. 5). The adsorption of PFOS and PFOA was fast at the initial stage, and most adsorption was finished within 12 h, followed by the slow adsorption until 24 h. It is noticeable that PFOS adsorption was much faster than PFOA at the initial stage, and the adsorbed amount of PFOS was also much higher than that of PFOA. The pseudo-second-order model [23] described the adsorption kinetic data of PFOS and PFOA on the bamboo-derived GAC very well ($R^2 > 0.98$), and the initial adsorption velocity (v_0) was 1.43 mmol/g/h for PFOS and 0.37 mmol/g/h for PFOA. Some granular adsorbents were also used to remove PFOS and PFOA in the literature, but much longer time was required to reach the adsorption equilibrium due to the slow diffusion of PFOS/PFOA in the intraparticle pores. For example, the commercial anion-exchange resins with different functional groups and matrixes required 48–168 h to reach the sorption equilibrium for PFOS [9]; the commercially available GAC needed over 168 h to achieve the sorption equilibrium for both PFOS and PFOA [7]; the crosslinked chitosan beads required about 24–100 h to reach the adsorption equilibrium for PFOS at pH ranging from 3.0 to 9.5 [11]. Evidently, the bamboo-derived GAC had the relatively fast adsorption for PFOS and PFOA among the granular adsorbents. Since the bamboo-derived GAC had many macropores (Fig. 4), the diffusion of PFOS/PFOA in the GAC was fast. However, only about 4 h was required to achieve the adsorption equilibrium of PFOS and PFOA on the powdered activated carbon [7].

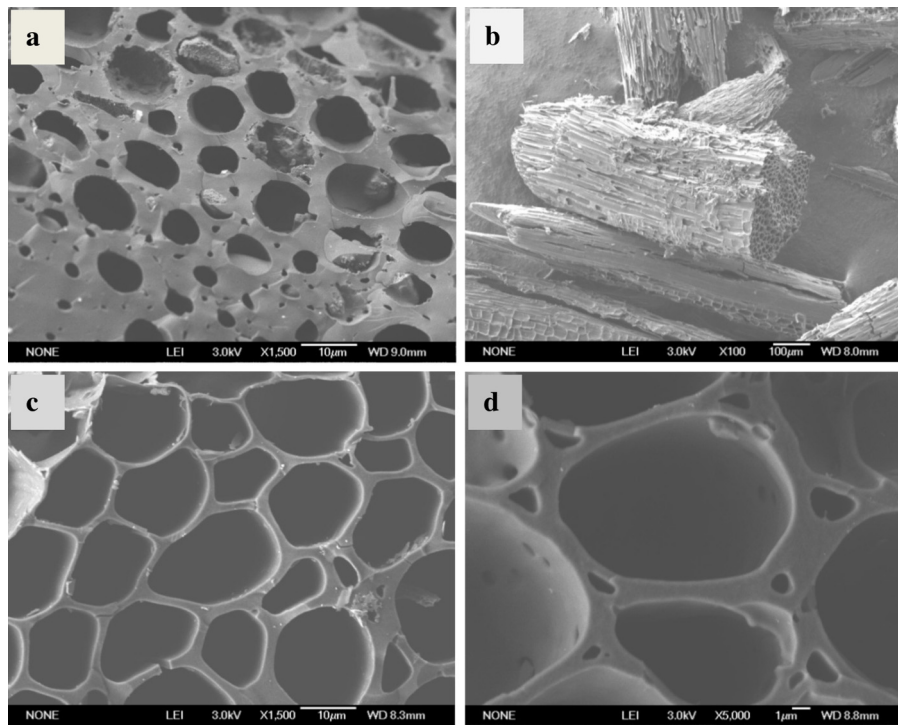


Fig. 4. SEM images of carbonized bamboo (a), bamboo-derive activated carbon at the magnitude of $\times 100$ (b), $\times 1500$ (c), and $\times 5000$ (d).

3.5. Effect of solution pH

Fig. 6a presents the effect of solution pH on the adsorption of PFOS and PFOA on the bamboo-derived GAC. When solution pH increased from 3.0 to 10.0, the adsorbed amounts of PFOA decreased significantly at pH below 6 and then decreased slowly. In contrast, the adsorbed amounts of PFOS decreased rapidly with increasing pH from 3 to 4, and decreased very slowly at pH above 4. The zeta potentials of the adsorbent surfaces at different solution pH values are shown in Fig. 6b, and the point of zero charge of the activated carbon was found to be at about pH 3.2. Since the value of pK_a is -3.27 for PFOS [24,25] and 2.5 for PFOA [26], PFOS should all exist as anions at pH above 3.0 and about 50% of PFOA species are anions at pH 2.5. The electrostatic attraction should be involved in the adsorption of PFOS on the bamboo-derived GAC at pH below 3.2, while the electrostatic repulsion should occur between PFOS anions and negatively charged activated carbon at pH above 3.2. For PFOA, some neutral molecules may adsorb on the activated carbon via the hydrophobic interaction at pH below 5, but they gradually changed into anions with increasing solution pH from 3.0 to 6.0 and

would not adsorb on the negatively charged activated carbon due to the electrostatic repulsion, resulting in the significant decrease of PFOA adsorption at pH from 3.0 to 6.0.

Although the electrostatic repulsion prevented the adsorption of PFOS/PFOA on the activated carbon at pH above 3.2, their adsorbed amounts were still high (Fig. 6a), indicating that other interactions were involved in the adsorption. In consideration of the hydrophobicity of PFOS and PFOA, they may adsorb on the activated carbon via hydrophobic interaction. We measured the

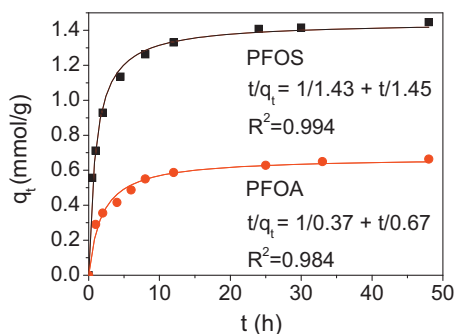


Fig. 5. Sorption kinetics of PFOS and PFOA on the bamboo-derived GAC and modeling results using the pseudo-second-order equation ($t/q_t = 1/\nu_0 + t/q_e$, ν_0 represents the initial sorption rate, and q_e is the adsorbed amount at equilibrium).

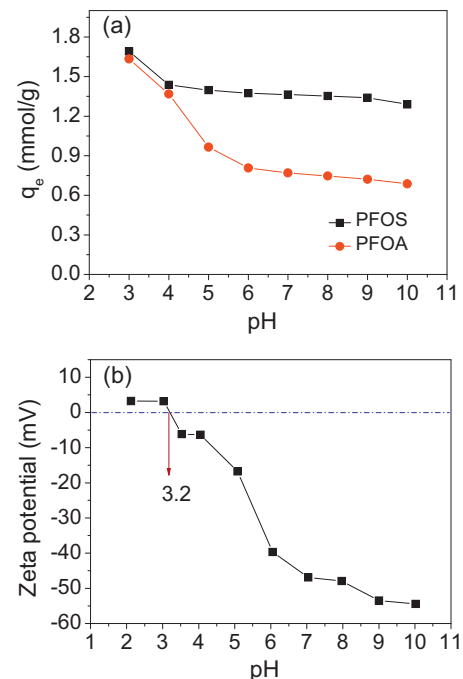


Fig. 6. Effect of pH on PFOS/PFOA adsorption (a) and zeta potentials (b) on the bamboo-derived activated carbon.